Proceedings of APCC2015 copyright © 2015 IEICE 14 SB 0087

Identification of Inter-Cell Uplink Interferers based on Multi-Cell Scheduling Matrix Inversion

Thomas Bourgeois*, Kazuhide Toda*, Takeo Ohseki*, Toshiaki Yamamoto†, Yasuhiro Suegara*
*KDDI R&D Laboratories Inc. (2-1-15 Ohara, Fujimino-shi, Saitama, 356-8502 Japan)
{th-bourgeois, ku-toda, ohseki, ya-suegara}@kddilabs.jp
†KDDI Corporation. (3-10-10 Iidabashi, Chiyoda-ku, Tokyo, 102-0072 Japan)
{to-yamamoto}@kddi.com

***Abstract*—In this paper, we present a new technique to identify the main inter-cell uplink interferers at each base station of a cellular network simultaneously. In the proposed scheme, for the duration of the interferer identification process, the scheduling of all users to uplink transmission resources is determined by a central controller. The scheduling is carefully chosen so that each cell can determine the contribution of each interferer from measurements of total received interference power by inversion of the interferer scheduling matrix. The advantages of the proposed scheme are as follows. Firstly, it can be adapted to any physical layer and take advantage of a central controller (a widely expected 5G feature). Secondly, it can be operated in both time-division duplex (TDD) and frequency-division duplex (FDD) modes and scales well with the network density. Finally, all the complexity is placed on the base station side, thus reducing the pressure on the user terminal's hardware. The effectiveness of the method is demonstrated mathematically and its performances are investigated by means of Monte-Carlo simulations. Results show that the proposed technique performs as well as the conventional method based on quantized reports of downlink measurements used in LTE-Advanced.**

I. Introduction

The launch of new wireless applications (e.g traffic control, remote driving, industrial robots, free-viewpoint camera, smart grid, "Internet-of-Things", etc) in the near future is conditioned by the ability of the underlying networks to handle the corresponding increase in traffic. Given the expected growth in the coming years of the existing fleet of wirelessly connected devices in both size and diversity, the current LTE-Advanced (4G) networks will be unable to meet the spatial capacity (i.e $bit/s/m^2$) requirements set by these new applications [1]. A direct solution to this spatial capacity issue is to increase spatial reuse through the deployment of dense networks of inter-connected small cells [2], [3]. Nevertheless, inter-cell interference mitigation techniques which scale well with the cell density are necessary in order to exploit the benefits of densification. In this paper, we focus on the case of uplink inter-cell interference. Most works related to uplink inter-cell interference focus on techniques, such as interference alignment and power control, to be applied once interferers are already identified and ranked by interference strength [4]–[6]. However, up to our knowledge, there is a lack of research on techniques targeting the identification and ranking of users from neighbor cells by level of mean interference power. The two main existing techniques are as follows. 1) The first consists in designing Sounding Reference Signals (SRS) orthogonal between cells and then operating a joint multi-cell SRS scheduling (as suggested in [7]). However, the number of orthogonal sequences is limited, therefore the technique does not scale with the cell density. 2) The second technique consists in exploiting measurement reports of downlink Reference Signal Received Power (RSRP), as in [8]. This is the only approach currently implemented in LTE-Advanced. However, this method employs quantized measurement reports and is limited by the user terminal processing capabilities[1]. Finally, the technique does not fit well the case of Frequency-Division Duplex, where uplink and downlink may have significantly different propagation characteristics.

In this paper, we present a new technique to identify the main sources of inter-cell uplink interference at each base station of the network simultaneously. The advantages of the proposed scheme are as follows. Firstly, it takes into account advanced multi-cell coordination via a central controller (a widely expected 5G feature) and can be adapted to any type of physical layer. Secondly, it can be operated in both time-division duplex (TDD) and frequency-division duplex (FDD) modes and scales satisfyingly with the network size and the network density. Finally, all the complexity is placed on the base station side, thus reducing the pressure on the hardware of the user terminal. The remainder of this paper is organized as follows. In section II, the main concepts and the system model used for the analysis are introduced. In section III, the proposed scheme is presented in details and its feasibility is demonstrated mathematically for a particular physical layer implementation. In section IV, by means of Monte-Carlo simulations, we evaluate the performance of the proposed scheme in terms of the percentage of identified interference power with respect to the total received interference power. Finally, in section V a conclusion summarizes the paper.

II. Basic Idea & System Requirements

A. Deployment & transceiver assumptions

We consider an arbitrarily large two-dimensional homogeneous wireless network with a spatial density of base station λ_{BS} and a spatial density of user λ_U. All cells each have one base station are assumed to share the same frequency band and to be connected to a same central controller. The proposed scheme can be implemented in both TDD and FDD. Without loss of generality, all users and all base stations are assumed to be equipped with a single omnidirectional antenna. Although the technique can be easily adapted to any FFT/IFFT-based

[1]User terminals detect the signals from multiple base stations using Successive Interference Cancellation (SIC), the performance thereof is fundamentally limited by the noise figure of the receiver. [9]

Proceedings of APCC2015 copyright © 2015 IEICE 14 SB 0087

multi-carrier scheme, we assume the uplink physical layer to implement OFDM (e.g OFDMA or SC-FDMA). The set of time samples corresponding to the output of an IFFT operation plus its Cyclic Prefix (CP) are denoted as an OFDM symbol. Users are assumed to be moving but slowly enough so that the following two conditions are true. 1) The coherence time T_{coh} of the channel spans multiple OFDM symbols. 2) The path-loss on each link appears constant over a duration T_{PL} much longer than the duration T_{obs} of the observation window during which the interferer identification process takes place.

B. Scheduling matrix: definition & properties

Considering the plane $\mathcal{P}$ of time-frequency transmission resources available to the system, a logical scheduling resource (LSR) is defined as a collection of non-empty regions of $\mathcal{P}$. In the remainder of the paper, we will only consider the case of orthogonal LSRs (i.e non overlapping). Given a set $\mathcal{M}$ of $M = |\mathcal{M}|$ LSRs[2] and a set $\mathcal{U}$ of $U = |\mathcal{U}|$ users, a scheduler is a mapping from $\mathcal{U}$ to $\mathcal{M}$. The scheduler can be completely described by a binary matrix $\mathbf{S}$ of size $M \times U$ such that $(\mathbf{S})_{m,u} = 1$ (resp. $(\mathbf{S})_{m,u} = 0$) if the u-th user is active (resp. inactive) on the m-th LSR. We define such a matrix $\mathbf{S}$ as a scheduling matrix. In the remainder of this paper, scheduling matrices will be denoted as $\mathbf{S}_{\mathcal{M},\mathcal{U}}$. If $M \geq U$ (i.e, the matrix is 'slim') and the columns of $\mathbf{S}_{\mathcal{M},\mathcal{U}}$ are linearly independent, then given two vectors $\mathbf{x}, \mathbf{y}$, the linear system $\mathbf{y} = \mathbf{S}_{\mathcal{M},\mathcal{U}}\mathbf{x}$ associated with $\mathbf{S}_{\mathcal{M},\mathcal{U}}$ admits a unique solution $\mathbf{x}_{LS}$ in the least-square sense (or has an exact unique solution $\mathbf{x}_E$ if $M = U$). Considering a given cell c_0, we define the Neighbor Cell Cluster (NCC) of c_0 as the set of its L closest neighbor cells denoted by $\mathcal{C}_{c_0} = \{c_1, c_2, ..., c_L\}$, where L is chosen so that the users connected to these L cells, denoted by the set $\mathcal{I}_{c_0}$, are responsible for most of the interference received at cell c_0 (e.g. $> 95\%$). We assume in the remainder that the same size L is used for all cells. In the next subsections, we show how, given a set of LSRs $\mathcal{M}$, the knowledge of $\mathbf{S}_{\mathcal{M},\mathcal{I}_{c_0}}$ at c_0 allows it to determine the individual average interference power contribution of each user in $\mathcal{I}_{c_0}$.

C. Scheduling matrix inversion & interferer identification

It is clear that the fading-averaged received power in a given LSR is a function of the combination of the users transmitting on it. Consider a collection of non over-lapping sets of M LSRs each denoted as $\mathcal{M}_1^P = \{\mathcal{M}_1, \mathcal{M}_2, ..., \mathcal{M}_P\}$ spanning the whole observation window. Then, let us assume that a given cell c_0 can decode its own users scheduled on each LSR of $\mathcal{M}_1^P$ and that $\mathcal{I}_{c_0}$ is scheduled such that $\mathbf{S}_{\mathcal{M}_1,\mathcal{I}_{c_0}} = \mathbf{S}_{\mathcal{M}_2,\mathcal{I}_{c_0}} = ... = \mathbf{S}_{\mathcal{M}_P,\mathcal{I}_{c_0}} = \mathbf{S}_{\mathcal{M}_1^P,\mathcal{I}_{c_0}}$. In the remainder of this paper, we call the matrix $\mathbf{S}_{\mathcal{M}_1^P,\mathcal{I}_{c_0}}$ of size $M \times |\mathcal{I}_{c_0}|$ the Interferer Scheduling Matrix (ISM) of cell c_0. Figure 1 illustrates the relation between the ISM and the scheduling of each cell's own users. The rows of an ISM are called received interferer combinations (RIC) and its columns are scheduling vectors (SV). After decoding and subtraction of its own users on all scheduled LSRs within the observation window, cell c_0 can determine the vector $\widehat{\mathbf{P}}_{Rx}$ which contains an estimate of the mean received interference power corresponding to each RIC. Then, if the ISM is 'slim' and full-rank, cell c_0 can estimate the vector $\widehat{\mathbf{P}}_{\mathcal{I}_{c_0}}$, which contains the individual interference power contribution of each user in $\mathcal{I}_{c_0}$, by solving the linear system $\widehat{\mathbf{P}}_{Rx} = \mathbf{S}_{\mathcal{M}_1^P,\mathcal{I}_{c_0}}\mathbf{P}_{\mathcal{I}_{c_0}}$. This enables cell c_0 to better select targets for its interference mitigation techniques. It should be noted that ISMs can be made full-rank as long as some LSRs are left unused by some cells. Simulations show that the average fraction of unused LSRs can easily be set as low as $5 \sim 10\%$. In summary, for T_{obs} seconds, the system employs a particular non-channel dependent scheduler (non-CDS) enabling the use of the proposed interferer identification technique. The acquired knowledge may be used for $T_{PL} - T_{obs}$ seconds for targeted interference management (TIM). If the Signal-to-Noise-plus-Interference Ratio (SINR) gain from TIM is large enough, it compensates the lower throughput imposed during the observation window, leading to a net throughput gain in average.

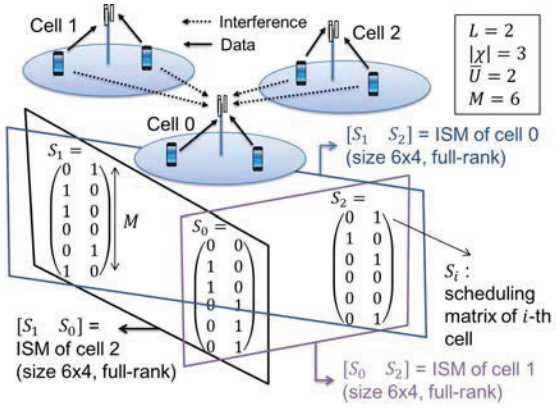

Fig. 1. shows a scheduling allocation enabling the use of the proposed technique at all cells simultaneously. For clarity, each cell has only two connected users and only cell 0's interfering links are illustrated with arrows.

D. Scheduling matrix allocation

Since we consider a network of arbitrarily large size, it is not possible for the central controller to attribute a different SV to each connected user. Indeed, since the ISM of each cell must be 'slim', this would require an arbitrarily large number of LSRs to be devoted to the interferer identification process. In order to minimize the number of LSRs required, linearly independent SVs must be spatially reused as much as possible. Solving this problem can be done using a graph coloring approach as follows. 1) Construct the graph formed by selecting the base stations as vertices and creating an edge between each base station and its L nearest neighbor base stations. 2) Find a coloring of this graph and denote the set of colors used as $\mathcal{X}$. Then, 3) for each color $x \in \mathcal{X}$, determine $W_x = \min\left(\overline{U}, \max_{c \in \mathcal{C}_x}(U_c)\right)$ where $\mathcal{C}_x$ is the set of cells attributed with the color x and $\overline{U}$ is the maximum number of distinct users a cell is allowed to schedule during the interferer identification process. 4) Attribute a same set $\mathcal{S}_x$ of W_x SVs to each cell in $\mathcal{C}_x$, so that the union of these sets denoted $\mathcal{S} = \bigcup_{x \in \mathcal{X}} \mathcal{S}_x$ forms a family of $W = \sum_{x \in \mathcal{X}} W_x$ linearly independent vectors. This implies that the matrix formed by this family of SVs is of size $M \times W$ with

$$M \geq W = \sum_{x \in \mathcal{X}} \min\left(\overline{U}, \max_{c \in \mathcal{C}_x}(U_c)\right) \quad (1)$$

[2]The notation $|.|$ represents the cardinal operator when applied to a discrete set and the absolute value operator when applied to a scalar.

Proceedings of APCC2015 copyright © 2015 IEICE 14 SB 0087

For example, in figure 1, $|\mathcal{X}| = 3$ colors are used and each cell is given $\overline{U} = 2$ SVs.

III. Mathematical analysis: The case of distributed subcarrier mapping

A. Physical mapping of Logical Scheduling Resources

The mathematical analysis focuses on the case of a distributed mapping of the subcarriers reserved to each uplink user. In a distributed subcarrier mapping, the subcarriers of each user are spread over the whole system bandwidth at fixed interval, thus creating a comb-like pattern which provides the best averaging of fast fading in the frequency domain. Simultaneous multiple access is enabled through the use of multiple non-overlapping combs of subcarriers. In more details, in each cell of the network, connected users are separated in G scheduling groups (SG). All users in the system placed in the same SG use the same exact comb of subcarriers, independently of the cell in which they are located. The combs associated to different SGs are separated by a frequency-shift of one subcarrier, as illustrated in figure 2. To improve averaging of fading at the receiver, the spacing Δf between two adjacent active subcarriers of a given comb should be chosen such that $\Delta f \geq \max(\rho_f B_{coh}, G\delta f)$, where δf is the subcarrier bandwidth, B_{coh} is the coherence bandwidth of the system and $\rho_f > 1$ is an arbitrary constant. The number of active subcarriers is the same for all combs and is denoted as K. Therefore, the total number of subcarriers used in the system is GK. A LSR is mapped to all the subcarriers associated with the user's scheduling group over N consecutive OFDM symbols and thus contains NK modulation symbols. The G SGs are considered to form G distinct uplink multiple access channels due to the orthogonality of their underlying scheduling resources. The scheduling matrix allocation process described in the previous section should be done separately for each SG and the parameter $\overline{U}$ is defined per SG. In the remainder of this section, stated results are considered to apply to any of the G SGs and thus the index g is dropped.

B. Measurement averaging & channel model

One sample of received interference power for a given RIC is obtained from exactly one LSR. Therefore, the duration required to obtain such a sample is NT_{OFDM}. The sampling period T_{samp} for a given RIC is set at a minimum of $\rho_t T_{coh}$ (where $\rho_t > 1$ is an arbitrary constant) to ensure independent fading between different samples (see figure 2). The M RICs are time-multiplexed so that P samples are obtained for each of them within the total observation window. Given M RICs, the time between two samples of a same RIC is given by $T_{samp} \geq \max(T_{coh}, MNT_{OFDM})$. Therefore, the maximum number of samples P per RIC is $\left\lfloor \frac{T_{obs}}{\max(T_{coh}, MNT_{OFDM})} \right\rfloor$.

The influence of the environment on the propagation of transmitted signals is assumed to be captured by a power law path-loss function and a normalized complex block-fading model accounting for fast variations in the amplitude and phase of the received signal. The path-loss function is defined as the bijection $r \rightarrow r^{-\alpha}$, where α is the path-loss exponent and r is the inter-node distance. Regarding fading, the time-frequency plane is divided into blocks each spanning T_{coh} seconds and B_{coh} Hertz. In each block, fast fading is modeled by a single frequency-domain complex circularly-symmetric Gaussian random variable h with zero mean and unit variance (i.e $h \sim \mathcal{CN}(0,1)$). At the receiver, the noise in each frequency-domain received symbol is modeled by a complex circularly-symmetric Gaussian random variable with zero mean and variance σ_w^2.

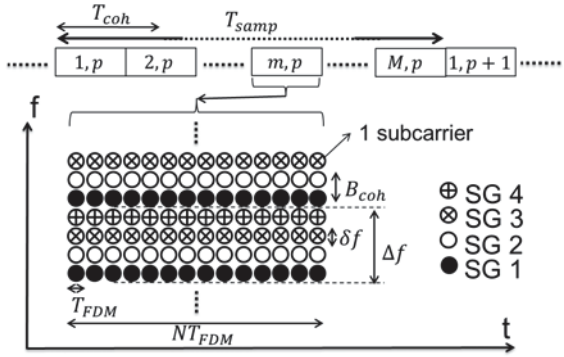

Fig. 2. shows the structure of the physical layer considered in section III for the case of $G = 4$ SGs. For clarity, only the resources for a single RIC are illustrated.

C. Average interference power estimation: receiver processing

Let us denote as $\mathcal{U}$ the set of all the $|\mathcal{U}| = U$ users located in a given SG. Let $\mathcal{M}_1^P$ be the collection of P sets of M LSRs each corresponding to the region of the time-frequency plane devoted to the interferer identification process. Let $\mathbf{S}_{\mathcal{M}_1^P,\mathcal{U}}$ denote the scheduling matrix of size $M \times U$ mapping $\mathcal{U}$ to $\mathcal{M}_1^P$. Let the user connected to cell c_0 be given the index $u = 0$, the users in $\mathcal{I}_{c_0}$ be given the indexes $\{1, 2, ..., |\mathcal{I}_{c_0}|\}$ and the other users be given the indexes $u > |\mathcal{I}_{c_0}|$. Let $P_u = P_{Tx} r_{c_0,u}^{-\alpha}$ where $r_{c_0,u}$ is the distance between the u-th user and cell c_0 and P_{Tx} is the terminal's transmit power, which is assumed the same for all users. Let $\widetilde{z}_{m,p}(n,k)$ be the frequency-domain complex symbol at a given base station c_0 on the k-th subcarrier during the n-th OFDM symbol of the LSR used to produce the p-th sample of the m-th RIC after the decode-and-subtract process of cell c_0 own user's signal. Let the term $h_{m,p,u}(k)$ be the corresponding complex channel gain, $d_{m,p,u}(n,k)$ be a constant-amplitude complex data symbol and $w_{m,p}(n,k)$ be the complex noise term. To model the imperfect decoding and subtraction of c_0's own user's signal, we model the residue from this step as a complex circularly-symmetric Gaussian random variable distributed as $\epsilon_{m,p}(n,k) \sim \mathcal{CN}\left(0, \xi P_0 \left(\mathbf{S}_{\mathcal{M}_1^P,\mathcal{U}}\right)_{m,0}\right)$ where $\xi \in [0;1]$ [10]. In average, each cell's own users benefit from positive decibel-scale SINRs. In such case, proper channel coding and rate adaptation can enable error-free detection. Then, the only source of error left in the decode-and-subtract process is the channel estimation (CE) error. Therefore, we have $\xi = MSE_{eq}$ where MSE_{eq} is the mean-square error (MSE) of the CE process. We assume that $\epsilon_{m,p}(n,k)$ is independent from the thermal noise and express their sum as $\tilde{w}_{m,p}(n,k) = \epsilon_{m,p}(n,k) + w_{m,p}(n,k)$ It follows that

Proceedings of APCC2015 copyright © 2015 IEICE 14 SB 0087

$\widetilde{z}_{m,p}(n,k)$ can then be written as

$$\widetilde{z}_{m,p}(n,k) = \tilde{w}_{m,p}(n,k) + \sum_{u\in\mathcal{I}_{c_0}} \sqrt{P_u}\left(\mathbf{S}_{\mathcal{M}_1^P,\mathcal{I}_{c_0}}\right)_{m,u} h_{m,p,u}(k)\, d_{m,p,u}(n,k) + \sum_{u>|\mathcal{I}_{c_0}|} \sqrt{P_u}\left(\mathbf{S}_{\mathcal{M}_1^P,\mathcal{U}}\right)_{m,u} h_{m,p,u}(k)\, d_{m,p,u}(n,k) \quad (2)$$

Taking the squared magnitude of all the symbols $\widetilde{z}_{m,p}(n,k)$ and then averaging over the K subcarriers and over the N OFDM symbols, we obtain the p-th time sample of total interference power for the m-th RIC, which we denote $\widetilde{P}_{Rx,m,p} = \frac{1}{NK}\sum_{n,k}|\widetilde{z}_{m,p}(n,k)|^2$. After collecting P samples for each of the M RICs, the time-averaged total interference power per RIC is calculated as $\widetilde{P}_{Rx,m} = \frac{1}{P}\sum_{p=1}^{P}\widetilde{P}_{Rx,m,p}$ $(m = 1,2,...,M)$. Let us denote $\widetilde{\mathbf{P}}_{Rx} = \left[\widetilde{P}_{Rx,1},\widetilde{P}_{Rx,2},...,\widetilde{P}_{Rx,M}\right]^T$, $\mathbf{P}_{\mathcal{I}_{c_0}} = \left[P_1,P_2,...,P_{|\mathcal{I}_{c_0}|}\right]^T$ and $\mathbf{P}_{\overline{\mathcal{I}}_{c_0}} = \left[\xi P_0, P_{1+|\mathcal{I}_{c_0}|}, P_{2+|\mathcal{I}_{c_0}|},...,P_U\right]^T$. One can reasonably assume that the channel coefficients $h_{m,p,u}(k)$, the data symbols $d_{m,p,u}(n,k)$ and noise samples $\tilde{w}_{m,p,u}(n,k)$ are all independent from one another across all indexes n,k,m,p,u. Then, assuming ergodicity of these processes, as the number of averaged symbols grows large the cross-correlation terms fade away and we thus obtain

$$\widetilde{\mathbf{P}}_{Rx} \rightarrow \mathbf{S}_{\mathcal{M}_1^P,\mathcal{I}_{c_0}}\mathbf{P}_{\mathcal{I}_{c_0}} + \underbrace{\mathbf{S}_{\mathcal{M}_1^P,\{0,\overline{\mathcal{I}}_{c_0}\}}\mathbf{P}_{\overline{\mathcal{I}}_{c_0}} + \sigma_w^2\mathbf{I}}_{\mathbf{Y}} \quad (3)$$

where $\mathbf{I}$ is the identity matrix and $\mathbf{Y}$ denotes the undesirable term. In practice, selecting proper Δf and T_{samp} enables to approach this ideal case sufficiently to obtain exploitable results. The term $\mathbf{Y}$ can actually be estimated given knowledge of the cells's positions, of the propagation characteristics of the environment and of the employed hardware. In this paper, we assume that $\widehat{\mathbf{Y}}$ the estimate of $\mathbf{Y}$ only accounts for the receiver noise power. It follows that an estimate $\widehat{\mathbf{P}}_{\mathcal{I}_{c_0}}$ of $\mathbf{P}_{\mathcal{I}_{c_0}}$ can then be obtained by the least-square method as

$$\widehat{\mathbf{P}}_{\mathcal{I}_{c_0}} = \left(\mathbf{S}^T_{\mathcal{M}_1^P,\mathcal{I}_{c_0}}\mathbf{S}_{\mathcal{M}_1^P,\mathcal{I}_{c_0}}\right)^{-1}\mathbf{S}^T_{\mathcal{M}_1^P,\mathcal{I}_{c_0}}\left(\widetilde{\mathbf{P}}_{Rx} - \widehat{\mathbf{Y}}\right) \quad (4)$$

where $\mathbf{S}^T$ and $\mathbf{S}^{-1}$ denote the transpose and inverse of a matrix $\mathbf{S}$, respectively.

IV. Simulation-based performance evaluation

In this section, we evaluate the performance of the proposed technique by means of Monte-Carlo computer simulations. The maximum number of simultaneous targets of interference mitigation techniques is typically very limited [11]. Therefore, it is paramount for a cell c_0 able to cancel a maximum of A_{max} interferers to identify the top-A_{max} users from $\mathcal{I}_{c_0}$ with highest average interference power. For a given cell c_0, let $P_{\overline{\{c_0\}}}$ be the total average interference power at c_0 from all users active during the interference identification process but not connected to c_0. Also let $\mathcal{A}_{c_0} \subset \mathcal{I}_{c_0}$ be the set of $\min(A_{max}, |\mathcal{I}_{c_0}|)$ users which have been identified by cell c_0 and let $P_{\mathcal{A}_{c_0}}$ be the total average interference power at c_0 from these identified users. The interference from the users in $\mathcal{A}_{c_0}$ is deemed actionable (i.e, can be acted on), since some techniques can target its sources to reduce it. The Ratio of Actionable Interference (denoted γ_{RAI}) of cell c_0 is thus defined as $\gamma_{RAI} = \frac{P_{\mathcal{A}_{c_0}}}{P_{\overline{\{c_0\}}}}$. The parameter γ_{RAI} is used as a performance metric in order to compare the proposed technique to three reference cases. 1) The first one, called 'ideal' case, is such that each cell c_0 knows perfectly the order of users in $\mathcal{I}_{c_0}$ sorted by decreasing average interference power and thus can always select correctly the top-A_{max} strongest interferers as targets for interference mitigation techniques. 2) The second case, called 'RSRP' case, corresponds to the conventional technique currently implemented in LTE-Advanced networks. 3) In the third case used for comparison, called the 'static information' case, cells do not perform any interferer identification and only rely on static information about the distance between base stations.

TABLE I. Fixed Simulation Parameters

Parameter	Symbol	Value
path-loss exponent	α	3.5
user density	λ_{UE}	700 node/km^2
base station density	λ_{BS}	20 node/km^2
bandwidth	B	10 MHz
carrier frequency	f_c	2 GHz
user speed	v	3 km/h
mean rms delay	τ_{rms}	$0.25\mu s$
max. num. of scheduled users	$\overline{U}$	20 user/cell/SG
num. of SGs	G	6
size of NCC	L	10 cells

The RSRP-based method used for comparison is defined as follows. All UEs connected to a cell are assumed to report perfect estimates, quantized with Q bits, of the path-loss between them and their L_{RSRP} closest neighbor cells (including their serving cell). These reports are processed by a central controller to identify and rank the uplink interferers of each cell. The infinite homogeneous network is approximated by a square of sufficient size (i.e, determined as in [12]). The performance of the cell closest to the center of the square are recorded. Physical layer and deployment parameters are chosen as close as possible to the 3GPP specification for LTE-Advanced dense small cell scenarios [13] (i.e. each LSR lasts 1 ms and $N = 14$). The modulation used for data symbols is QPSK and we set $P = 1$[3]. Numerical values for other fixed parameters are summarized in table I. The 50% coherence time and coherence bandwidth are $T_{coh} = \sqrt{\frac{9c^2}{16\pi f_c^2 v}}$ and $B_{coh} = \frac{1}{5\tau_{rms}}$, respectively, where v is the user's speed and τ_{rms} is the average root-mean-square (rms) delay of the system [14]. To ensure the fading coefficients at all the received symbols are sufficiently uncorrelated, we set $\rho_t = 2$ and $\rho_f = 2$. The resulting observation window spans $T_{obs} = 300$ ms.

In figure 3, γ_{RAI} performances of the different schemes are compared, given $Q = 7$ bits[4]. The parameter ξ is assumed to be equal to the MSE of the CE process. The mapping of SINR to CE MSE given in [15] is used to obtain realistic

[3]The distributed subcarrier mapping used here already provides sufficient averaging of fading so that higher values of P only provide negligible performance gain in the given setup. Note that other LSR mappings may require $P > 1$ to obtain sufficient averaging of fading.

[4]For comparison, in LTE-Advanced, the reported RSRP can take one of 98 values from -140 dBm to -44 dBm, which also requires 7 bits.

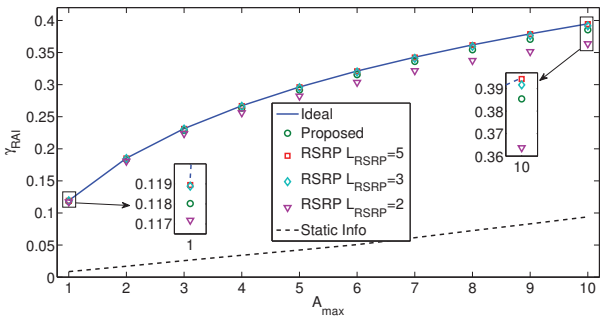

Fig. 3. γ_{RAI} at a cell c_0 as a function of $A_{max} = |\mathcal{A}_{c_0}|$ for various cases.

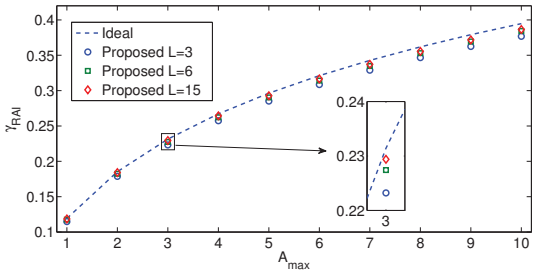

Fig. 4. γ_{RAI} at a cell c_0 as a function of $A_{max} = |\mathcal{A}_{c_0}|$ for various values of L.

values of ξ[5]. We observe that although the RSRP scheme performs better than the proposed scheme for $L_{RSRP} > 2$, both of them achieve performances close to the ideal case. The proposed scheme performance is affected by the imperfect decode-and-subtract process and by interference from users outside of the NCC. In figure 4, we observe that most of the performance is already achieved for $L = 3$, which indicates we may reduce T_{obs} to some extent while preserving a given γ_{RAI}. Nonetheless, as the RSRP case employs CDS at all time, it is still likely to outperform the proposed scheme in terms of average net throughput gain. While this latter may represent an important metric for smartphone-dominated 4G networks, a 5G network composed in a large part of low-rate, constant-traffic, machine-type devices will put more emphasis on hardware complexity and power consumption. In such case, the proposed technique represents an attractive alternative to the RSRP case.

V. Conclusion

In this paper, we presented a new technique for the identification of uplink inter-cell interference sources in a cellular system. The proposed scheme exploits a central controller to control the scheduling of each cell in a given set of time-frequency resources. The scheduling is carefully chosen so that each cell can determine the contribution of each interferer from measurements of total received interference power by inversion of the interferer scheduling matrix. The feasibility of the technique is demonstrated mathematically for a conventional frequency-division multiplexing physical layer implementation. The advantages of the proposed scheme are as follows. Firstly, it can be adapted to various physical layers. Secondly, it can be operated in both time-division duplex (TDD) and frequency-division duplex (FDD) modes and scales satisfyingly with the network size and the network density. Finally, all the complexity is placed on the base station side, thus reducing the pressure on the user terminal hardware. Performance results confirmed by computer simulations show that the proposed technique performs as well as the conventional method based on quantized report of Downlink measurements. In a future work, we will investigate the proposed technique in terms of practical performance metrics relevant to 5G networks and identify the most likely use cases.

[5]Although [15] focuses on LTE-Advanced downlink, CRS-based CE has a behavior close to that of uplink CE in the case of distributed subcarrier mapping and its performance is thus used as reference.

References

[1] A. Osseiran, F. Boccardi, V. Braun, K. Kusume, P. Marsch, M. Maternia, O. Queseth, M. Schellmann, H. Schotten, H. Taoka, H. Tullberg, M. Uusitalo, B. Timus, and M. Fallgren, "Scenarios for 5g mobile and wireless communications: the vision of the metis project," *Communications Magazine, IEEE*, vol. 52, no. 5, pp. 26–35, May 2014.

[2] T. Levanen, J. Pirskanen, and M. Valkama, "Dense small-cell networks: Rethinking the radio interface beyond lte-advanced," in *5G for Ubiquitous Connectivity (5GU), 2014 1st International Conference on*, Nov 2014, pp. 163–169.

[3] M. Condoluci, M. Dohler, G. Araniti, A. Molinaro, and K. Zheng, "Toward 5g densenets: architectural advances for effective machine-type communications over femtocells," *Communications Magazine, IEEE*, vol. 53, no. 1, pp. 134–141, January 2015.

[4] K. Balachandran, J. Kang, K. Karakayali, and K. Rege, "Network-centric cooperation schemes for uplink interference management in cellular networks," *Bell Labs Technical Journal*, vol. 18, no. 2, pp. 23–36, Sept 2013.

[5] K. Lee, "Uplink interference alignment for two-cell mimo interference channels," *Vehicular Technology, IEEE Transactions on*, vol. 62, no. 4, pp. 1861–1865, May 2013.

[6] Y. Sun, R. Jover, and X. Wang, "Uplink interference mitigation for ofdma femtocell networks," *Wireless Communications, IEEE Transactions on*, vol. 11, no. 2, pp. 614–625, February 2012.

[7] E. Dahlman, S. Parkvall, and J. Skld, "Chapter 11 - uplink physical-layer processing," in *4G: LTE/LTE-Advanced for Mobile Broadband (Second Edition)*, second edition ed., E. D. P. Skld, Ed. Oxford: Academic Press, 2014, pp. 241 – 297. [Online]. Available: http://www.sciencedirect.com/science/article/pii/B9780124199859000118

[8] K. Oltmann, R. Cavalcante, S. Stanczak, and M. Kasparick, "Interference identification in cellular networks via adaptive projected subgradient methods," in *Signals, Systems and Computers, 2013 Asilomar Conference on*, Nov 2013, pp. 1946–1950.

[9] Y. Shen, T. Luo, and M. Win, "Neighboring cell search for lte systems," *Wireless Communications, IEEE Transactions on*, vol. 11, no. 3, pp. 0908–919, March 2012.

[10] A. Hasan and J. Andrews, "Cancellation error statistics in a power-controlled cdma system using successive interference cancellation," in *Spread Spectrum Techniques and Applications, 2004 IEEE Eighth International Symposium on*, Aug 2004, pp. 419–423.

[11] J. Andrews, "Interference cancellation for cellular systems: a contemporary overview," *Wireless Communications, IEEE*, vol. 12, no. 2, pp. 19–29, April 2005.

[12] M. Haenggi and R. K. Ganti, "Interference in large wireless networks," *Found. Trends Netw.*, vol. 3, no. 2, pp. 127–248, Feb. 2009. [Online]. Available: http://dx.doi.org/10.1561/1300000015

[13] 3rd Generation Partnership Project (3GPP); Technical Specification Group Radio Access Network, "Small cell enhancements for e-utra and e-utran - physical layer aspects (release 12)," Tech. Rep. 36.872 V1.0.0, August 2007.

[14] T. S. Rappaport, *Wireless Communications: Principles & Practice*, 2nd ed. Prentice-Hall:Upper Saddle River, 2002.

[15] M. Meidlinger and Q. Wang, "Performance evaluation of lte advanced downlink channel estimators," in *Systems, Signals and Image Processing (IWSSIP), 2012 19th International Conference on*, April 2012, pp. 252–255.